



Research article

Ultraspherical spectral collocation method for two-dimensional tempered space-fractional Zeldovich–Frank–Kamenetskii equations with exponential nonlinearities

M.A. Zaky^{1,*}, M.Z. Youssef¹, A. Al Kenany² and S.S. Ezz-Eldien^{3,4,*}

¹ Department of Mathematics and Statistics, College of Science, Imam Mohammad Ibn Saud Islamic University (IMSIU), P.O. Box-65892, Riyadh 11566, Saudi Arabia

² Mathematics Department, Al-Qunfudah University College, Umm Al-Qura University, Mecca, KSA

³ Department of Mathematics, Faculty of Science, New Valley University, El-Kharga, 72511, Egypt

⁴ Department of Information Technology, Faculty of Computer and Information, Socotra Archipelago University, Socotra, Yemen

* **Correspondence:** Email: ma.zaky@yahoo.com, s_sezeldien@yahoo.com.

Abstract: This paper introduces a novel spectral collocation method for solving two-dimensional tempered space-fractional Zeldovich–Frank–Kamenetskii (ZFK) equations, which generalize the classical combustion model by incorporating tempered fractional diffusion operators. The tempered fractional ZFK equation is pivotal for modeling anomalous diffusion phenomena in thermal reaction and combustion systems, where nonlocal interactions and memory effects play a critical role. The proposed hybrid numerical scheme combines a spectral collocation method based on ultraspherical polynomials for spatial discretization with an implicit Runge–Kutta (IRK) technique for temporal integration. For the first time, we derive new tempered fractional differentiation matrices in physical space using ultraspherical polynomial bases, enabling efficient handling of the nonlocal tempered fractional operators. The results highlight the effectiveness of the new differentiation matrices in capturing anomalous diffusion phenomena while maintaining spectral accuracy, providing a robust framework for fractional combustion modeling.

Keywords: tempered fractional derivative; Zeldovich–Frank–Kamenetskii equations; spectral method; ultraspherical polynomials

Mathematics Subject Classification: 34A08, 65M70, 33C45

1. Introduction

Differential equation models with exponential nonlinearity appear in many fields of mathematics, ranging from models of earthquake faulting [2] to plastic deformation in metals [11] and electrical oscillators [17]. These nonlinear terms are not solely physical but also serve mathematical purposes, such as regularizing non-smooth systems via smooth approximations like tanh functions [18], analyzing gene regulatory networks that converge exponentially to piecewise-smooth limiting systems [15], and employing singular exponential coordinates in tropical geometry to study algebraic systems [19]. While exponential nonlinearities address threshold behaviors and regularization, another layer of complexity arises in systems requiring nonlocal memory effects, a domain where fractional calculus has emerged as a critical tool.

Although fractional calculus is not a relatively new science, its fundamentals and principles have been extensively studied for decades [24, 25]. With an increasing number of natural phenomena that can be accurately described using various types of fractional differential equations [10, 20], many researchers remain interested in developing fractional calculus and developing numerous definitions and properties that will help to make new contributions to this important field. Tempered fractional differentiation is considered one of the most recent and important definitions of fractional differentiations, given its ability to describe some phenomena that traditional fractional differentiation definitions cannot explain. Introducing an exponential smoothing factor into the fractional differentiation helps control the influence of distant past events, offering an advantage in studying systems with exponential memory decay, such as geophysical flows [21], groundwater hydrology [22], finance [5], and poroelasticity [13]. Zaky [29] studied the existence and uniqueness of a class of tempered fractional differential equations, and applied the spectral collocation scheme for its numerical solution. Obeidat and Benteil [23] investigated the existence and uniqueness of the solution to the tempered fractional Black-Scholes and tempered fractional convection-diffusion equations, making use of the tempered fractional natural transform approach. Saffarian and Mohebbi [28] introduced a stable semi-discrete numerical method based on the finite difference scheme followed by the Crank–Nicolson approach in the time direction and the finite element method in the space direction for getting an unconditionally stable numerical solution for one- and two-dimensional time–space fractional tempered diffusion-wave equations. Rayal and Verma [27] implemented an operational technique with the spectral collocation method for the numerical solution of a tempered fractional Klein–Gordon equation based on two–dimensional Gegenbauer wavelets. In [3], Bu and Oosterlee employed the shifted Grünwald difference methods as the basis of a third-order semi-discretized numerical approach to solve the tempered fractional diffusion equation. Qiao et al. [26] introduced a numerical solution to the multidimensional tempered fractional integrodifferential equation using the second-order convolution quadrature and backward differentiation schemes in the time direction, with implicit and finite difference approaches in the alternating direction in the space direction. The authors in [12] utilized the Fox H-function to derive the analytical solution of the one-dimensional tempered fractional diffusion equation, and then they applied a graded mesh L_1 -based Galerkin finite element approach for the solution of a two-dimensional tempered time–space fractional diffusion equation.

Reaction-diffusion equations play an important role in modeling many natural phenomena in physics, ecology, chemistry, and biology [7–9]. Furthermore, fractional reaction–diffusion equations are known to be flexible tools for describing complex systems that exhibit nonlocal behavior or memory

effects, something classical reaction-diffusion equations cannot do (see [1, 6, 14]). As a special kind of reaction–diffusion equation, the ZFK equation provides an accurate interpretation to the combustion theory; it helps model the propagation of planar laminar premixed flames [4, 16]. While significant progress has been made in numerical methods for tempered fractional reaction–diffusion equations, existing schemes predominantly address linear or polynomial nonlinearities, leaving a critical gap in handling systems with exponential reaction terms, which are central to combustion models like the ZFK equations. Extensions to two-dimensional tempered fractional ZFK equations, which couple anomalous diffusion with stiff exponential nonlinearities of the form $\frac{\lambda^2}{2}\nu(1-\nu)e^{-\lambda(1-\nu)}$, remain absent in prior work. This paper fills this gap by introducing a spectral collocation method that combines ultraspherical polynomial bases for spatial discretization with IRK time integration. The approach explicitly addresses the computational challenges of the exponential nonlinearity and derives tempered fractional differentiation matrices in physical space, enabling efficient resolution in two-dimensional geometries. By unifying spectral accuracy for tempered operators with robust time stepping, the method provides the first dedicated framework for simulating two-dimensional tempered fractional ZFK equations.

The main contribution of this paper is highlighted as follows:

- Ultraspherical polynomials are employed for the first time as basis functions in the numerical solution of tempered fractional ZFK equations.
- Tempered fractional differentiation matrices are derived in physical space using ultraspherical polynomial bases.
- A hybrid spectral–temporal framework is developed by combining ultraspherical discretization with IRK time integration.
- The application of the spectral collocation approach is validated through numerical experiments on benchmark problems.

The paper is outlined as follows: Section 2 introduces some basic tools and definitions. Section 3 presents a numerical solution to the two–dimensional tempered space–fractional ZFK equation using the spectral collocation approach. Section 4 discusses the application of the IRK method to the resulting system of ordinary differential equations. Section 5 obtains the numerical results to ensure the validity of the presented numerical scheme. Section 6 provides some concluding remarks.

2. Preliminaries

This section introduces the foundational mathematical concepts and tools necessary for the subsequent analysis, including definitions of fractional operators and properties of ultraspherical polynomials.

2.1. Fractional operators

This subsection defines the Riemann–Liouville (RL) fractional derivatives and their tempered variants, which are crucial for modeling the nonlocal dynamics in the tempered fractional ZFK equation. Key operators include left/right derivatives and their tempered extensions, culminating in the fractional diffusion operator.

The left RL fractional derivative is defined as

$${}_0D_x^\vartheta v(x, t) = \frac{1}{\Gamma(n - \vartheta)} \frac{\partial^n}{\partial x^n} \int_0^x \frac{v(\tau, t)}{(x - \tau)^{\vartheta - n + 1}} d\tau, \quad n - 1 < \vartheta < n, \quad (2.1)$$

where $\Gamma(\cdot)$ is the gamma function, n is an integer, and ϑ is the fractional order.

The right RL fractional derivative is given by

$${}_xD_\ell^\vartheta v(x, t) = \frac{(-1)^n}{\Gamma(n - \vartheta)} \frac{\partial^n}{\partial x^n} \int_x^\ell \frac{v(\tau, t)}{(\tau - x)^{\vartheta - n + 1}} d\tau, \quad n - 1 < \vartheta < n. \quad (2.2)$$

The left RL tempered fractional derivative extends the classical RL derivative by incorporating an exponential tempering factor γ . It is defined as

$${}_0D_x^{\vartheta, \gamma} v(x, t) = \frac{e^{-\gamma x}}{\Gamma(n - \vartheta)} \frac{\partial^n}{\partial x^n} \int_0^x \frac{e^{\gamma \tau} v(\tau, t)}{(x - \tau)^{\vartheta - n + 1}} d\tau, \quad n - 1 < \vartheta < n, \quad (2.3)$$

where $\gamma > 0$ is the tempering parameter that controls the exponential decay.

Similarly, the right RL tempered fractional derivative is defined as

$${}_xD_\ell^{\vartheta, \gamma} v(x, t) = \frac{(-1)^n e^{\gamma t}}{\Gamma(n - \vartheta)} \frac{\partial^n}{\partial x^n} \int_x^\ell \frac{e^{-\gamma \tau} v(\tau, t)}{(\tau - x)^{\vartheta - n + 1}} d\tau, \quad n - 1 < \vartheta < n. \quad (2.4)$$

The variants of the left and right RL tempered fractional derivatives are defined as

$$\partial_{+x}^{\vartheta, \gamma} v(x, t) = {}_0D_x^{\vartheta, \gamma} v(x, t) - \gamma^\vartheta v(x, t) - \vartheta \gamma^{\vartheta - 1} \frac{\partial v}{\partial x}(x, t)$$

and

$$\partial_{-x}^{\vartheta, \gamma} v(x, t) = {}_xD_\ell^{\vartheta, \gamma} v(x, t) - \gamma^\vartheta v(x, t) + \vartheta \gamma^{\vartheta - 1} \frac{\partial v}{\partial x}(x, t),$$

The fractional diffusion operator, which combines the left and right variants, is defined as

$$\partial_{|x|}^{\vartheta, \gamma} v(x, t) = -\frac{1}{2 \cos(\vartheta \pi / 2)} \left(\partial_{-x}^{\vartheta, \gamma} v(x, t) + \partial_{+x}^{\vartheta, \gamma} v(x, t) \right).$$

2.2. Ultraspherical polynomials

This subsection outlines the properties of ultraspherical polynomials, their orthogonality, recurrence relations, and quadrature rules. These polynomials form the basis for the spectral discretization method, enabling efficient approximation and differentiation in bounded domains.

The ultraspherical polynomials, denoted as $\mathcal{G}_k^\theta(z)$ with $\theta > -\frac{1}{2}$, form a complete orthogonal system on the interval $[-1, 1]$. These polynomials satisfy the recurrence relation

$$k\mathcal{G}_k^\theta(z) = 2(k + \theta - 1)z\mathcal{G}_{k-1}^\theta(z) - (k + 2\theta - 2)\mathcal{G}_{k-2}^\theta(z), \quad k = 2, 3, \dots,$$

with initial conditions $\mathcal{G}_0^\theta(z) = 1$ and $\mathcal{G}_1^\theta(z) = 2\theta z$. The explicit polynomial form of $\mathcal{G}_k^\theta(z)$ is given by the series expansion

$$\mathcal{G}_k^\theta(z) = \sum_{m=0}^k \frac{\Gamma(\theta + \frac{1}{2})\Gamma(2\theta + k + m)}{\Gamma(2\theta)\Gamma(m + \theta + \frac{1}{2})m!(k - m)!} \left(\frac{z - 1}{2} \right)^m.$$

The orthogonality of these polynomials is expressed through the weighted orthogonality relation

$$\int_{-1}^1 \mathcal{G}_k^\theta(z) \mathcal{G}_l^\theta(z) w^\theta(z) dz = h_k^\theta \delta_{kl},$$

where the weight function is $w^\theta(z) = (1 - z^2)^{\theta - \frac{1}{2}}$ and the normalization constant is

$$h_k^\theta = \frac{\pi 2^{1-2\theta} \Gamma(2\theta + k)}{k!(k + \theta) \Gamma^2(\theta)}.$$

For polynomial interpolation, the quadrature rule is

$$\int_{-1}^1 \phi(z) w^\theta(z) dz = \sum_{j=0}^{\aleph} w_{\aleph,j}^\theta \phi(z_j),$$

where the nodes z_j include the endpoints $z_0 = -1$ and $z_\aleph = 1$ and the interior nodes are the zeros of $\partial_z \mathcal{G}_\aleph^{(\theta)}(z)$ for $j = 1, \dots, \aleph - 1$. The corresponding weights are

$$w_{\aleph,0}^\theta = w_{\aleph,\aleph}^\theta = \frac{2^{-1+2\theta} (1 + 2\theta) \Gamma\left(\frac{1}{2} + \theta\right)^2 \Gamma(\aleph)}{\Gamma(1 + 2\theta + \aleph)},$$

$$w_{\aleph,j}^\theta = \frac{2^{-1-2\theta} \pi \Gamma(2\theta + \aleph)}{\Gamma(1 + \theta) \Gamma(2 + \theta) \Gamma(\aleph) \mathcal{G}_{-2+\aleph}^{1+\theta}(z_j) \mathcal{G}_{-2+\aleph}^{2+\theta}(z_j) (1 - z_j^2)}.$$

Any function $u(z, t) \in L_{w^\theta}^2([-1, 1])$ can be approximated by the series expansion

$$u(z, t) = \sum_{k=0}^{\infty} \sum_{l=0}^{\infty} c_{kl} \mathcal{G}_k^\theta(z) \mathcal{G}_l^\theta(z),$$

where the coefficients c_{kl} are computed as

$$c_{kl} = \frac{1}{h_k^\theta h_l^\theta} \int_{-1}^1 \int_{-1}^1 u(z, t) \mathcal{G}_k^\theta(z) \mathcal{G}_l^\theta(z) w^\theta(z) dz dt.$$

3. Two-dimensional spectral discretization

In this section, we present a spatial discretization approach for the tempered fractional ZFK equation using the pseudospectral collocation method combined with expansions in ultraspherical polynomials along the spatial dimension. The equation under consideration is

$$\frac{\partial v}{\partial t}(x, y, t) - \epsilon \partial_{|x|}^{\theta, \gamma} v(x, y, t) - \epsilon \partial_{|y|}^{\theta, \gamma} v(x, y, t) = \frac{\lambda^2}{2} v(x, y, t) (1 - v(x, y, t)) e^{-\lambda(1-v(x,y,t))} + p(x, y, t), \quad (3.1)$$

where $(x, y) \in \Omega = (0, \ell_x) \times (0, \ell_y)$ and $t \in I = (0, T]$. The boundary and initial conditions are given by

$$v(0, y, t) = v(\ell_x, y, t) = v(x, 0, t) = v(x, \ell_y, t) = 0, \quad \text{for } t \in I, \text{ on } \partial\Omega,$$

$$v(x, y, 0) = g(x, y), \quad \text{on } \Omega,$$

where $1 < \vartheta < 2$ and $\gamma > 0$.

The solution $v(x, y, t)$ is expressed in terms of unknown variable coefficients $\hat{v}_{s,r}(t)$ as follows:

$$v(x, y, t) = \sum_{s=0}^{\mathfrak{N}_x} \sum_{r=0}^{\mathfrak{N}_y} \hat{v}_{s,r}(t) \psi_s(x) \phi_r(y),$$

where $\psi_s(x)$ and $\phi_r(y)$ are the shifted ultraspherical polynomials defined on the physical domains $[0, \ell_x]$ and $[0, \ell_y]$, respectively. These basis functions are constructed from the standard ultraspherical polynomials $\mathcal{G}_s^\theta(\zeta)$ and $\mathcal{G}_r^\theta(\eta)$ defined on $[-1, 1]$ via the transformations:

$$\psi_s(x) = \mathcal{J}_s^\theta(\zeta(x)), \quad \text{where } \zeta(x) = \frac{2x}{\ell_x} - 1,$$

$$\phi_r(y) = \mathcal{J}_r^\theta(\eta(y)), \quad \text{where } \eta(y) = \frac{2y}{\ell_y} - 1.$$

These bases are orthogonal with respect to the weight functions $w^\theta(x)$ and $w^\theta(y)$ on $[0, \ell_x]$ and $[0, \ell_y]$, respectively. The orthogonality relations are given by:

$$(\psi_s(x), \psi_l(x))_w = \int_0^{\ell_x} \psi_s(x) \psi_l(x) w^\theta(x) dx = h_s^\theta \delta_{sl},$$

$$(\phi_r(y), \phi_k(y))_w = \int_0^{\ell_y} \phi_r(y) \phi_k(y) w^\theta(y) dy = h_r^\theta \delta_{rk}.$$

The normalization constants $h_{x,s}^\theta$ and $h_{y,r}^\theta$ for the shifted ultraspherical polynomials $\psi_s(x)$ and $\psi_r(y)$ are given by:

$$h_{x,s}^\theta = \frac{\pi \ell_x^{1-2\theta} \Gamma(2\theta + s)}{s!(s + \theta) \Gamma^2(\theta)},$$

$$h_{y,r}^\theta = \frac{\pi \ell_y^{1-2\theta} \Gamma(2\theta + r)}{r!(r + \theta) \Gamma^2(\theta)}.$$

The ultraspherical Gauss Lobatto (UGL) quadrature rule is applied in both spatial directions

$$\int_0^{\ell_x} \int_0^{\ell_y} \phi(x, y) w^\theta(x) w^\theta(y) dx dy = \sum_{i=0}^{\mathfrak{N}_x} \sum_{j=0}^{\mathfrak{N}_y} \varpi_{\mathfrak{N}_x, i}^\theta \varpi_{\mathfrak{N}_y, j}^\theta \phi(x_{\mathfrak{N}_x, i}, y_{\mathfrak{N}_y, j}).$$

The UGL nodes and weights in the x -direction are given by

$$x_{\mathfrak{N}_x, i} = \frac{\ell_x}{2} (1 + \zeta_i), \quad \varpi_{\mathfrak{N}_x, i}^\theta = \frac{\ell_x}{2} w_{\mathfrak{N}_x, i}^\theta, \quad i = 0, 1, \dots, \mathfrak{N}_x,$$

and these in the y -direction are given by

$$y_{\mathfrak{N}_y, j} = \frac{\ell_y}{2} (1 + \eta_j), \quad \varpi_{\mathfrak{N}_y, j}^\theta = \frac{\ell_y}{2} w_{\mathfrak{N}_y, j}^\theta, \quad j = 0, 1, \dots, \mathfrak{N}_y.$$

The spatial tempered fractional and integer–order derivatives are approximated using ultraspherical differentiation matrices in both x and y directions. For $x_{\mathfrak{N}_x, n}$ and $y_{\mathfrak{N}_y, m}$, the coefficients $\hat{v}_{s,r}(t)$ are computed via the discrete inner product:

$$\hat{v}_{s,r}(t) = \frac{1}{h_s^\theta h_r^\theta} \sum_{j=0}^{\mathfrak{N}_x} \sum_{k=0}^{\mathfrak{N}_y} \psi_s(x_{\mathfrak{N}_x, j}) \phi_r(y_{\mathfrak{N}_y, k}) \varpi_{\mathfrak{N}_x, j}^\theta \varpi_{\mathfrak{N}_y, k}^\theta v(x_{\mathfrak{N}_x, j}, y_{\mathfrak{N}_y, k}, t). \quad (3.2)$$

Spatial fractional derivatives are approximated using ultraspherical differentiation matrices. For $x_{\mathfrak{N}_x, n}$ ($n = 1, \dots, \mathfrak{N}_x - 1$) and $y_{\mathfrak{N}_y, m}$ ($m = 1, \dots, \mathfrak{N}_y - 1$)

$$\begin{aligned} {}_0D_x^{\theta, \gamma} v(x, y, t) &= \sum_{i=0}^{\mathfrak{N}_x} \sum_{j=0}^{\mathfrak{N}_y} \left(\sum_{k=0}^{\mathfrak{N}_x} \sum_{l=0}^{\mathfrak{N}_y} \frac{1}{h_k^\theta h_l^\theta} \psi_k(x_{\mathfrak{N}_x, i}) \phi_l(y_{\mathfrak{N}_y, j}) \right. \\ &\quad \left. \times \varpi_{\mathfrak{N}_x, i}^\theta \varpi_{\mathfrak{N}_y, j}^\theta {}_0D_x^{\theta, \gamma} [\psi_k(x)] \phi_l(y) \right) v(x_{\mathfrak{N}_x, i}, y_{\mathfrak{N}_y, j}, t), \end{aligned} \quad (3.3)$$

$$\begin{aligned} {}_x D_{\ell_x}^{\theta, \gamma} v(x, y, t) &= \sum_{i=0}^{\mathfrak{N}_x} \sum_{j=0}^{\mathfrak{N}_y} \left(\sum_{k=0}^{\mathfrak{N}_x} \sum_{l=0}^{\mathfrak{N}_y} \frac{1}{h_k^\theta h_l^\theta} \psi_k(x_{\mathfrak{N}_x, i}) \phi_l(y_{\mathfrak{N}_y, j}) \right. \\ &\quad \left. \times \varpi_{\mathfrak{N}_x, i}^\theta \varpi_{\mathfrak{N}_y, j}^\theta {}_x D_{\ell_x}^{\theta, \gamma} [\psi_k(x)] \phi_l(y) \right) v(x_{\mathfrak{N}_x, i}, y_{\mathfrak{N}_y, j}, t). \end{aligned} \quad (3.4)$$

At the nodes $x_{\mathfrak{N}_x, n}$ ($n = 1, \dots, \mathfrak{N}_x - 1$) and $y_{\mathfrak{N}_y, m}$ ($m = 1, \dots, \mathfrak{N}_y - 1$), we have

$${}_0D_x^{\theta, \gamma} v(x_{\mathfrak{N}_x, n}, y_{\mathfrak{N}_y, m}, t) = \sum_{i=0}^{\mathfrak{N}_x} \sum_{j=0}^{\mathfrak{N}_y} {}_L D_{i,j}^{n,m} v(x_{\mathfrak{N}_x, i}, y_{\mathfrak{N}_y, j}, t), \quad (3.5)$$

$${}_0D_y^{\theta, \gamma} v(x_{\mathfrak{N}_x, n}, y_{\mathfrak{N}_y, m}, t) = \sum_{i=0}^{\mathfrak{N}_x} \sum_{j=0}^{\mathfrak{N}_y} {}_L \bar{D}_{i,j}^{n,m} v(x_{\mathfrak{N}_x, i}, y_{\mathfrak{N}_y, j}, t), \quad (3.6)$$

$${}_x D_{\ell_x}^{\theta, \gamma} v(x_{\mathfrak{N}_x, n}, y_{\mathfrak{N}_y, m}, t) = \sum_{i=0}^{\mathfrak{N}_x} \sum_{j=0}^{\mathfrak{N}_y} {}_R D_{i,j}^{n,m} v(x_{\mathfrak{N}_x, i}, y_{\mathfrak{N}_y, j}, t), \quad (3.7)$$

$${}_y D_{\ell_y}^{\theta, \gamma} v(x_{\mathfrak{N}_x, n}, y_{\mathfrak{N}_y, m}, t) = \sum_{i=0}^{\mathfrak{N}_x} \sum_{j=0}^{\mathfrak{N}_y} {}_R \bar{D}_{i,j}^{n,m} v(x_{\mathfrak{N}_x, i}, y_{\mathfrak{N}_y, j}, t), \quad (3.8)$$

where

$${}_L D_{i,j}^{n,m} = \sum_{k=0}^{\mathfrak{N}_x} \sum_{l=0}^{\mathfrak{N}_y} \frac{1}{h_k^\theta h_l^\theta} \psi_k(x_{\mathfrak{N}_x, i}) \phi_l(y_{\mathfrak{N}_y, j}) \varpi_{\mathfrak{N}_x, i}^\theta \varpi_{\mathfrak{N}_y, j}^\theta {}_0D_{x_{\mathfrak{N}_x, n}}^{\theta, \gamma} [\psi_k(x_{\mathfrak{N}_x, n})] \phi_l(y_{\mathfrak{N}_y, m}), \quad (3.9)$$

$${}_L \bar{D}_{i,j}^{n,m} = \sum_{k=0}^{\mathfrak{N}_x} \sum_{l=0}^{\mathfrak{N}_y} \frac{1}{h_k^\theta h_l^\theta} \psi_k(x_{\mathfrak{N}_x, i}) \phi_l(y_{\mathfrak{N}_y, j}) \varpi_{\mathfrak{N}_x, i}^\theta \varpi_{\mathfrak{N}_y, j}^\theta \psi_k(x_{\mathfrak{N}_x, n}) {}_0D_{y_{\mathfrak{N}_y, m}}^{\theta, \gamma} [\phi_l(y_{\mathfrak{N}_y, m})], \quad (3.10)$$

$${}_R D_{i,j}^{n,m} = \sum_{k=0}^{\mathfrak{N}_x} \sum_{l=0}^{\mathfrak{N}_y} \frac{1}{h_k^\theta h_l^\theta} \psi_k(x_{\mathfrak{N}_x,i}) \phi_l(y_{\mathfrak{N}_y,j}) \varpi_{\mathfrak{N}_x,i}^\theta \varpi_{\mathfrak{N}_y,j}^\theta \psi_k(x_{\mathfrak{N}_x,n}) D_{\ell_x}^{\theta,\gamma} [\psi_k(x_{\mathfrak{N}_x,n})] \phi_l(y_{\mathfrak{N}_y,m}), \quad (3.11)$$

$${}_R \overline{D}_{i,j}^{n,m} = \sum_{k=0}^{\mathfrak{N}_x} \sum_{l=0}^{\mathfrak{N}_y} \frac{1}{h_k^\theta h_l^\theta} \psi_k(x_{\mathfrak{N}_x,i}) \phi_l(y_{\mathfrak{N}_y,j}) \varpi_{\mathfrak{N}_x,i}^\theta \varpi_{\mathfrak{N}_y,j}^\theta \psi_k(x_{\mathfrak{N}_x,n})_{y_{\mathfrak{N}_y,m}} D_{\ell_y}^{\theta,\gamma} [\phi_l(y_{\mathfrak{N}_y,m})]. \quad (3.12)$$

The tempered fractional diffusion derivative's spectral discretization can be represented in compact notation as

$$\partial_{|x|}^{\theta,\gamma} v(x_{\mathfrak{N}_x,n}, y_{\mathfrak{N}_y,m}, t) = \sum_{i=0}^{\mathfrak{N}_x} \sum_{j=0}^{\mathfrak{N}_y} \mathfrak{D}_{i,j}^{n,m} v(x_{\mathfrak{N}_x,i}, y_{\mathfrak{N}_y,j}, t) + \frac{\gamma^\theta}{\cos\left(\frac{\theta\pi}{2}\right)} v(x_{\mathfrak{N}_x,n}, y_{\mathfrak{N}_y,m}, t), \quad (3.13)$$

$$\partial_{|y|}^{\theta,\gamma} v(x_{\mathfrak{N}_x,n}, y_{\mathfrak{N}_y,m}, t) = \sum_{i=0}^{\mathfrak{N}_x} \sum_{j=0}^{\mathfrak{N}_y} \overline{\mathfrak{D}}_{i,j}^{n,m} v(x_{\mathfrak{N}_x,i}, y_{\mathfrak{N}_y,j}, t) + \frac{\gamma^\theta}{\cos\left(\frac{\theta\pi}{2}\right)} v(x_{\mathfrak{N}_x,n}, y_{\mathfrak{N}_y,m}, t), \quad (3.14)$$

where

$$\mathfrak{D}_{i,j}^{n,m} = -\frac{1}{2 \cos\left(\frac{\theta\pi}{2}\right)} \left({}_L D_{i,j}^{n,m} + {}_R D_{i,j}^{n,m} \right), \quad (3.15)$$

$$\overline{\mathfrak{D}}_{i,j}^{n,m} = -\frac{1}{2 \cos\left(\frac{\theta\pi}{2}\right)} \left({}_L \overline{D}_{i,j}^{n,m} + {}_R \overline{D}_{i,j}^{n,m} \right). \quad (3.16)$$

Let us denote

$$\begin{aligned} v_{i,j}(t) &= v(x_{\mathfrak{N}_x,i}, y_{\mathfrak{N}_y,j}, t), \\ p_{i,j}(t) &= p(x_{\mathfrak{N}_x,i}, y_{\mathfrak{N}_y,j}, t), \\ g_{i,j} &= g(x_{\mathfrak{N}_x,i}, y_{\mathfrak{N}_y,j}). \end{aligned}$$

As a result of these manipulations, we arrive at the following system of semi-discrete equations in time:

$$\begin{aligned} \dot{v}_{n,m}(t) &= \epsilon \sum_{i=1}^{\mathfrak{N}_x-1} \sum_{j=1}^{\mathfrak{N}_y-1} \mathfrak{D}_{i,j}^{n,m} v_{i,j}(t) + \epsilon \sum_{i=1}^{\mathfrak{N}_x-1} \sum_{j=1}^{\mathfrak{N}_y-1} \overline{\mathfrak{D}}_{i,j}^{n,m} v_{i,j}(t) \\ &+ \epsilon \frac{2\gamma^\theta}{\cos\left(\frac{\theta\pi}{2}\right)} v_{n,m}(t) + p_{n,m}(t) + \frac{\lambda^2}{2} v_{n,m}(t) (1 - v_{n,m}(t)) e^{-\lambda(1-v_{n,m}(t))}, \end{aligned} \quad (3.17)$$

with the initial condition

$$v_{n,m}(0) = g_{n,m}.$$

In fact, this allows for the exact imposition of boundary conditions

$$v_{0,k}(t) = v_{\mathfrak{N}_x,k}(t) = v_{j,0}(t) = v_{j,\mathfrak{N}_y}(t) = 0.$$

4. Implicit Runge–Kutta method

To solve the given system of differential equations numerically, we employ an IRK scheme. The system is described by

$$\frac{du_j}{dt} = F_j(t, u_1, \dots, u_{N-1}), \quad j = 1, \dots, N-1, \quad t \in (0, 1], \quad (4.1)$$

with the initial conditions

$$u_j(0) = h_j, \quad j = 1, \dots, N-1. \quad (4.2)$$

The solution is approximated using an IRK method. For a fixed time step size Δt , the discrete time points are defined as

$$t_n = t_0 + n\Delta t, \quad n = 0, 1, 2, \dots,$$

where $u_j^{(n)}$ denotes the numerical approximation of the exact solution $u_j(t_n)$.

The IRK scheme updates the solution iteratively as follows:

$$u_j^{(n+1)} = u_j^{(n)} + \Delta t \sum_{s=1}^p d_s \ell_{j,s}^{(n)}, \quad j = 1, \dots, N-1. \quad (4.3)$$

Here, the stage values $\ell_{j,s}^{(n)}$ are determined by solving the system

$$\ell_{j,s}^{(n)} = F_j(t_n + e_s \Delta t, R_{j,s}^{(n)}), \quad s = 1, \dots, p. \quad (4.4)$$

The intermediate approximations $R_{j,s}^{(n)}$ are computed as

$$R_{j,s}^{(n)} = u_j^{(n)} + \Delta t \sum_{r=1}^p f_{s,r} \ell_{j,r}^{(n)}, \quad s = 1, \dots, p. \quad (4.5)$$

In this formulation, Δt represents the step size, and the coefficients $f_{s,r}$, d_s , and e_s define the specific Runge–Kutta method. These coefficients are typically organized in the Butcher tableau as follows (Table 1):

Table 1. Butcher tableau for the IRK method.

e_1	f_{11}	\dots	f_{1p}
\vdots	\vdots	\ddots	\vdots
e_p	f_{p1}	\dots	f_{pp}
	d_1	\dots	d_p

5. Numerical results

In this example, we consider the two-dimensional tempered fractional ZFK equation on the domain $\Omega = [0, 1] \times [0, 1]$ with $\epsilon = 0.1$:

$$\frac{\partial v}{\partial t}(x, y, t) - \epsilon \partial_{|x|}^{\theta, \gamma} v(x, y, t) - \epsilon \partial_{|y|}^{\theta, \gamma} v(x, y, t) = \frac{1}{2} v(x, y, t) (1 - v(x, y, t)) e^{-(1-v(x, y, t))} + p(x, y, t). \quad (5.1)$$

The boundary and initial conditions are given by

$$v(0, y, t) = v(\ell_x, y, t) = v(x, 0, t) = v(x, \ell_y, t) = 0, \quad \text{for } t \in (0, 1], \text{ on } \partial\Omega.$$

$$v(x, y, 0) = x^3 y^3 (1 - x)^3 (1 - y)^3, \quad \text{on } \Omega.$$

The tempered fractional ZFK equation admits the exact solution $v(x, t) = e^{-t} x^3 (1 - x)^3 y^3 (1 - y)^3$.

To demonstrate the high-order accuracy and tempering sensitivity of the proposed method, we consider two characteristic cases:

- Without tempering ($\gamma = 0$): in Figure 1, the proposed method evaluates the space-fractional problem under negative tempering with fractional orders $\vartheta = 1.2, 1.6, \text{ and } 1.8$, Jacobi parameters $\theta = 2$ and $\beta = 2$, and spatial resolution $N = 10$, demonstrating high accuracy.
- Positive tempering ($\gamma = 1$): in Figure 2, the method achieves superior accuracy for all tested ϑ values, underscoring its adaptability to tempered fractional operators.

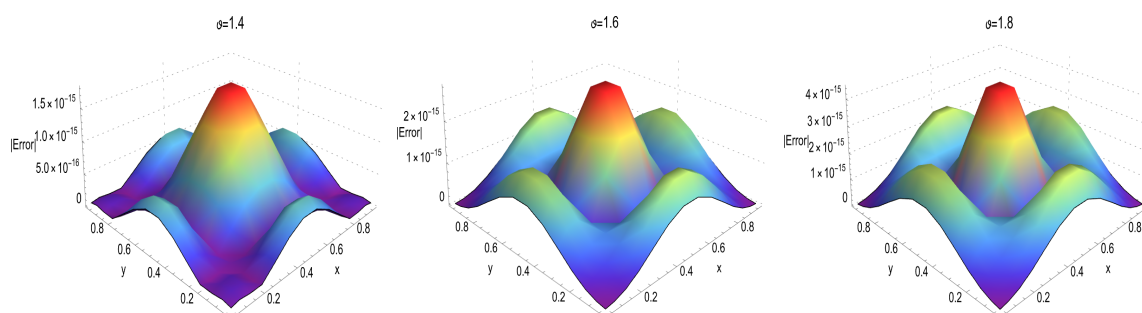


Figure 1. Absolute error function of u with $\gamma = 0$, $\theta = 2$, $N = 15$ and different values of ϑ .

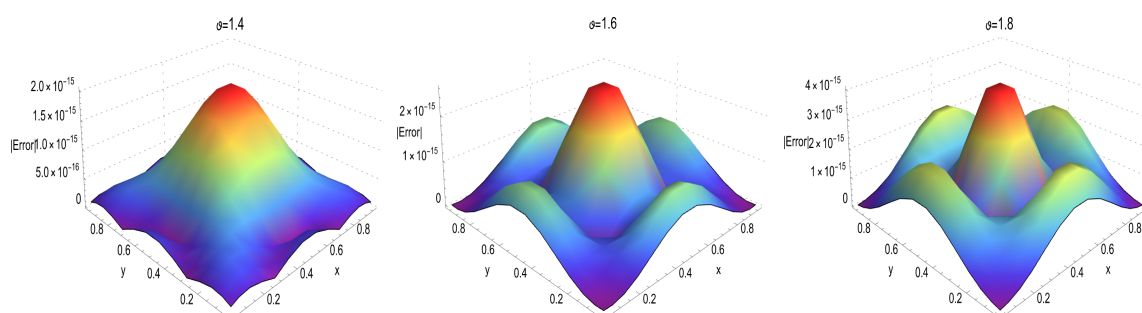


Figure 2. Absolute error function of u with $\gamma = 1$, $\theta = 2$, $N = 15$ and different values of ϑ .

6. Conclusions

This paper presented a high-order spectral discretization approach for solving the tempered fractional ZFK equation in two spatial dimensions. By introducing the differentiation matrices of ultraspherical polynomials, we developed a robust pseudospectral collocation framework capable of handling the non-local and tempered fractional operators efficiently. Central to this approach the use of shifted ultraspherical polynomials, which enabled accurate approximation of tempered fractional derivatives while inherently enforcing boundary conditions through the construction of the basis. The integration of Gauss-Lobatto quadrature ensured precise numerical differentiation and integration, maintaining spectral accuracy across the domain. Furthermore, the IRK scheme employed for temporal integration provided high-order accuracy.

Author contributions

M.A. Zaky: conceptualization, methodology, software; M.Z. Youssef: validation, visualization; A. Al Kenany: formal analysis, investigation; S.S. Ezz-Eldien: validation, visualization. All authors contributed to writing and revising the subsequent versions of the manuscript. All authors have read and approved the final version of the manuscript for publication.

Use of Generative-AI tools declaration

The authors declare they have not used Artificial Intelligence (AI) tools in the creation of this article.

Acknowledgments

This work was supported and funded by the Deanship of Scientific Research at Imam Mohammad Ibn Saud Islamic University (IMSIU) (grant number IMSIU-DDRSP2602).

Conflict of interest

The authors assert that they do not have any known competing financial interests or personal relationships that could have influenced the work reported in this paper.

References

1. M. Banerjee, M. Kuznetsov, O. Udovenko, V. Volpert, Nonlocal reaction-diffusion equations in biomedical applications, *Acta Biotheor.*, **70** (2022), 12. <https://doi.org/10.1007/s10441-022-09436-4>
2. E. Bossolini, M. Brøns, K. U. Kristiansen, Singular limit analysis of a model for earthquake faulting, *Nonlinearity*, **30** (2017), 2805. <https://doi.org/10.1088/1361-6544/aa712e>
3. L. Bu, C. W. Oosterlee, On high-order schemes for tempered fractional partial differential equations, *Appl. Numer. Math.*, **165** (2021), 459–481. <https://doi.org/10.1016/j.apnum.2021.03.008>

4. W. B. Bush, Asymptotic analysis of laminar flame propagation: review and extension, *Int. J. Eng. Sci.*, **17** (1979), 597–613. [https://doi.org/10.1016/0020-7225\(79\)90129-0](https://doi.org/10.1016/0020-7225(79)90129-0)
5. A. Cartea, D. Del-Castillo-Negrete, Fractional diffusion models of option prices in markets with jumps, *Phys. A*, **374** (2007), 749–763. <https://doi.org/10.1016/j.physa.2006.08.071>
6. W. Chen, L. Wu, Monotonicity and one-dimensional symmetry of solutions for fractional reaction-diffusion equations and various applications of sliding methods, *Ann. Mat. Pura Appl.*, **203** (2024), 173–204. <https://doi.org/10.1007/s10231-023-01357-4>
7. R. Cherniha, V. Davydovych, *Nonlinear reaction-diffusion systems*, Lecture Notes in Mathematics, Springer Cham, 2017. <https://doi.org/10.1007/978-3-319-65467-6>
8. C. Cosner, Reaction-diffusion equations and ecological modeling, In: *A. Friedman, Tutorials in mathematical biosciences IV*, Lecture Notes in Mathematics, Vol. 1922, Berlin: Heidelberg, 2008. https://doi.org/10.1007/978-3-540-74331-6_3
9. L. Dagdug, J. Pena, I. Pompa-Garcia, Reaction-diffusion equations, In: *Diffusion under confinement*, 2024, 361–395. https://doi.org/10.1007/978-3-031-46475-1_13
10. M. Dalir, M. Bashour, Applications of fractional calculus, *Appl. Math. Sci.*, **4** (2010), 1021–1032.
11. Y. Estrin, L. P. Kubin, Criterion for thermomechanical instability of low temperature plastic deformation, *Scripta Metallurgica*, **14** (1980), 1359–1364. [https://doi.org/10.1016/0036-9748\(80\)90195-7](https://doi.org/10.1016/0036-9748(80)90195-7)
12. L. Feng, F. Liu, V. V. Anh, Galerkin finite element method for a two-dimensional tempered time-space fractional diffusion equation with application to a Bloch–Torrey equation retaining Larmor precession, *Math. Comput. Simul.*, **206** (2023), 517–537. <https://doi.org/10.1016/j.matcom.2022.11.024>
13. A. Hanyga, Wave propagation in media with singular memory, *Math. Comput. Model.*, **34** (2001), 1399–1421. [https://doi.org/10.1016/S0895-7177\(01\)00137-6](https://doi.org/10.1016/S0895-7177(01)00137-6)
14. Y. Huang, Z. Wang, Analysis of tumor metastasis model in microenvironment based on coupled fractional reaction diffusion equation, *Comput. Math. Appl.*, **182** (2025), 24–45. <https://doi.org/10.1016/j.camwa.2025.01.012>
15. L. Ironi, L. Panzeri, E. Plahte, V. Simoncini, Dynamics of actively regulated gene networks, *Phys. D*, **240** (2011), 779–794. <https://doi.org/10.1016/j.physd.2010.12.010>
16. S. Jelbart, K. U. Kristiansen, P. Szmolyan, Traveling waves and exponential nonlinearities in the Zeldovich–Frank–Kamenetskii equation, *SIAM J. Appl. Dyn. Syst.*, **24** (2025), 530–556. <https://doi.org/10.1137/24M166200X>
17. S. Jelbart, K. U. Kristiansen, P. Szmolyan, M. Wechselberger, Singularly perturbed oscillators with exponential nonlinearities, *J. Dyn. Differ. Equ.*, **34** (2022), 1823–1875. <https://doi.org/10.1007/s10884-021-10041-1>
18. K. U. Kristiansen, Blowup for flat slow manifolds, *Nonlinearity*, **30** (2017), 2138. <https://doi.org/10.1088/1361-6544/aa6449>
19. K. U. Kristiansen, A. H. Sarantis, On a tropicalization of planar polynomial ODEs with finitely many structurally stable phase portraits, *arXiv Preprint*, 2023. <https://doi.org/10.48550/arXiv.2305.18002>

20. R. L. Magin, *Fractional calculus in bioengineering, part 1*, Begell House Inc., 2006. <https://doi.org/10.1615/CritRevBiomedEng.v32.i1.10>
21. M. M. Meerschaert, F. Sabzikar, M. S. Phanikumar, A. Zeleke, Tempered fractional time series model for turbulence in geophysical flows, *J. Stat. Mech. Theory Exp.*, **14** (2014), P09023. <https://doi.org/10.1088/1742-5468/2014/09/P09023>
22. M. M. Meerschaert, Y. Zhang, B. Baeumer, Tempered anomalous diffusion in heterogeneous systems, *Geophys. Res. Lett.*, **35** (2008), 1–5. <https://doi.org/10.1029/2008GL034899>
23. N. A. Obeidat, D. E. Benti, Novel technique to investigate the convergence analysis of the tempered fractional natural transform method applied to diffusion equations, *J. Ocean Eng. Sci.*, **8** (2023), 636–646. <https://doi.org/10.1016/j.joes.2022.05.014>
24. K. B. Oldham, J. Spanier, *The fractional calculus*, New York: Academic Press, 1974.
25. I. Podlubny, *Fractional differential equations*, San Diego, CA: Academic Press, 1999.
26. L. Qiao, J. Guo, W. Qiu, Fast BDF2 ADI methods for the multi-dimensional tempered fractional integrodifferential equation of parabolic type, *Comput. Math. Appl.*, **123** (2022), 89–104. <https://doi.org/10.1016/j.camwa.2022.08.014>
27. A. Rayal, S. R. Verma, Two-dimensional Gegenbauer wavelets for the numerical solution of tempered fractional model of the nonlinear Klein–Gordon equation, *Appl. Numer. Math.*, **174** (2022), 191–220. <https://doi.org/10.1016/j.apnum.2022.01.015>
28. M. Saffarian, A. Mohebbi, Solution of space-time tempered fractional diffusion-wave equation using a high-order numerical method, *J. Comput. Appl. Math.*, **423** (2023), 114935. <https://doi.org/10.1016/j.cam.2022.114935>
29. M. A. Zaky, Existence, uniqueness and numerical analysis of solutions of tempered fractional boundary value problems, *Appl. Numer. Math.*, **145** (2019), 429–457. <https://doi.org/10.1016/j.apnum.2019.05.008>



AIMS Press

©2026 the Author(s), licensee AIMS Press. This is an open access article distributed under the terms of the Creative Commons Attribution License (<https://creativecommons.org/licenses/by/4.0>)